

Change detection in Formosa satellite images via using Kullback-Leibler divergence

Li-Fen Huang (1), Yu-Lin Tsai (1), Shiau-Jing Liu (1)

¹National Space Organization, 8F, 9 Prosperity 1st Road, HsinChu, Taiwan
Email: evahuang@nspo.narl.org.tw; morphling@nspo.narl.org.tw;
cynthia@nspo.narl.org.tw.

KEY WORDS: Satellite Images, Kullback-Leibler Divergence, Change Detection Map, Hypothesis Testing

ABSTRACT: The satellite images, which can provide a time series data, are very useful to quickly detect spatial alteration for a large area. In order to get the change detection map, we propose a change detection algorithm for orthophoto based on Kullback-Leibler divergence (KL-div) and hypothesis testing in this paper. In the image, the list of pixel p is to sort the values of pixel p and its neighbors in numerical order. The list of pixel p (P) can be analogous to discrete probability distributions. For evaluating the KL-div between list of pixel p (P) and corresponding list of pixel q (Q) in the remote sensing images X_1 and X_2 with different time t_1 and t_2 , respectively, we define the following measurement

$$D_{KL}(p, q) = - \sum_i P(i) \log \left(\frac{Q(i)}{P(i)} \right) \quad (1)$$

The judgement method of change detection is based on hypothesis testing. In order to determine the change behavior, we propose the null hypotheses \mathcal{H}_0 and alternative hypotheses \mathcal{H}_1 are unchanged pixels and changed pixels, respectively. The conditional probability $P(p, q|\mathcal{H}_0)$ and $P(p, q|\mathcal{H}_1)$ of \mathcal{H}_0 and \mathcal{H}_1 can be defined by measuring the stand deviation of KL-div. After selecting a significance level, the null hypothesis will be rejected when the probability p-value is small than the significance level. Finally, the change detection map can be generated by proposed algorithm.

1. Introduction

In remote sensing application, the change detection, which is very useful to quickly detect spatial alteration for a large area, is one of the most interesting topic. The change detection is a useful technique for the environmental protection and the post-disaster analysis. The processing of the change detection is to identify the change data set which collects significantly different pixel between two satellite images with different obtained time. The change data set of satellite image has several underlying factors: (1) objects appearance/disappearance, (2) cloud, (3) shadow, (4) brightness, (5) accuracy of orthophoto, etc. The processing of change detection can be classified into three parts: (1) radiometric adjustment, (2) difference image generator, and (3) judgement. The radiance of satellite image is changed by the several factor such as season, solar angle, atmosphere condition, etc. There are several techniques to compensate the radiance difference. The simplest radiometric normalization processing, which is to match mean μ_1 and standard deviation σ_1 of the image X_1 and mean μ_2 and standard deviation σ_2 of

the image X_2 , respectively, is proposed by Dai and Khorram (Dai, 1998). The processing is based on the assumption that the images have Gaussian distribution. The radiometric normalization processing can be expressed by

$$X_2(u, v) = \frac{\sigma_1}{\sigma_2}(X_2(u, v) - \mu_2) + \mu_1 \quad (2)$$

In another way, the radiometric adjustment can be eliminated by computing the surface reflectance which contains information about the earth's surface. The surface reflectance can be estimated by two approach: (1) digital image processing method (Toth, 2000) and (2) physical model (Vermote, 2015). In the digital image processing approach, the observed image irradiance $X(u, v)$ at pixel (u, v) can be formulated

$$X(u, v) = X_{solar}(u, v)R(u, v) \quad (3)$$

Where $X_{solar}(u, v)$ is the irradiance from the sun at pixel (u, v) and $R(u, v)$ is the surface reflectance at pixel (u, v) . In order to extract surface reflectance $R(u, v)$, the homomorphic filter is used by assuming that the sun irradiance $X_{solar}(u, v)$ is low spatial frequency component. The irradiance $X_{solar}(u, v)$ and surface reflectance $R(u, v)$ can be separated by using logarithm

$$\ln X(u, v) = \ln X_{solar}(u, v) + \ln R(u, v) \quad (4)$$

The surface reflectance $\ln R(u, v)$ can be extraction by using high-pass filter F_{high_pass} . The approximate surface reflectance can be expressed

$$R(u, v) = \exp\{F_{high_pass}(\ln X(u, v))\} \quad (5)$$

In the physical model, the Second Simulation of a Satellite Signal in the Solar Spectrum (6S) is to formulate radiative transfer. The radiative transfer between satellite and observed target is simulated via realistic atmosphere model, anisotropic surfaces, and estimated gaseous absorption. Therefore, the surface reflectance can be accurate measured.

The simplest difference image generator is $D(u, v) = X_2(u, v) - X_1(u, v)$. This generator is widely used for quickly detecting image change in a short time (Skifstad, 1986). Skifstad and Jain proposed difference image generator via considering the variance of two image ratio $X_2(u, v)/X_1(u, v)$. The difference image $D(u, v)$ can be expressed

$$D(u, v) = \frac{1}{N} \sum_{(u,v) \in \Omega(u,v)} \left(\frac{X_2(u,v)}{X_1(u,v)} - \mu(u, v) \right)^2 \quad (6)$$

where Ω, u, v . is a block of pixels centered at $, u, v$. and μ, u, v . is defined by

$$\mu(u, v) = \frac{1}{N} \sum_{(u,v) \in \Omega(u,v)} \frac{X_2(u,v)}{X_1(u,v)} \quad (7)$$

The judgement can be simply defined by the following rule

$$J(u, v) = \begin{cases} 1 & \text{if } |D(u, v)| > \tau \\ 0 & \text{otherwise} \end{cases} \quad (8)$$

The threshold τ is chosen by different criteria according to application (Rosin, 1998). In this paper, we consider that the radiometric adjustment, difference image generator, and judgement are the simplest radiometric normalization processing, Kullback-Leibler Divergence, and hypothesis testing, respectively, for detecting change of Formosa satellite images.

2. Methodology

In this study, we want to detect change between Formosat-2 image X_1 and Formosat-5 image X_2 . Formosat-2 image and Formosat-5 image exists histogram distribution difference and quantization difference. We apply Equation (2) to eliminate the difference between Formosat-2 image and Formosat-5 image.

2.1 Difference image generator

We consider that the changes are associated with localized information. Therefore, the distance $D(u, v)$ between image $X_1(u, v)$ and image $X_2(u, v)$ is defined by $\Omega_1(u, v)$ and $\Omega_2(u, v)$ which are square block of pixels centered at (u, v) in each of the two images. The list of pixel p (P) is defined by

$$P = \{p_0, p_1, \dots, p_n\} \quad (9)$$

where $p_i = X_1(\hat{u}, \hat{v})$ for $(\hat{u}, \hat{v}) \in \Omega_1(u, v)$ with condition $p_i \geq p_j$ when $i < j$. There may exist pixel shift between image X_1 and image X_2 . To ensure that the corresponding square block of pixels in image X_1 and image X_2 are matched correctly, we assume that square block of pixels centered at (u, v) and square block of pixels centered at $(u + du, v + dv)$ in image X_1 and image X_2 , respectively, are corresponding square block. The shift pixel du and dv are satisfied $-N \leq du \leq N$ and $-M \leq dv \leq M$, respectively. Therefore, the list of pixel q (Q) is defined by

$$Q = \{q_0, q_1, \dots, q_n\} \quad (10)$$

where $q_i = X_2(\hat{u}, \hat{v})$ for $(\hat{u}, \hat{v}) \in \Omega_2(u + du, v + dv)$ with condition $q_i \geq q_j$ when $i < j$. KL-div between list of pixel p (P) and corresponding list of pixel q (Q) is defined by Equation (1) (Kullback, 1951). The Equation (1) is not symmetric distance ($D_{KL}(p, q) \neq D_{KL}(q, p)$). Therefore, we consider that a symmetric KL-div at (u, v) is expressed by

$$D_{SKL}(p, q) = D_{KL}(p, q) + D_{KL}(q, p) \quad (11)$$

The difference image $D(u, v)$ can be defined by

$$D(u, v) = \min_{\substack{-N \leq du \leq N \\ -M \leq dv \leq M}} D_{SKL}(p, q) \quad (12)$$

2.2 Judgement

The hypothesis testing is a straightforward judgement method of change detection for ignoring the noise effect. The tests of significance on the difference image $D(u, v)$ is to assess that null hypotheses \mathcal{H}_0 at each pixel is supported or rejected. To determine the change behavior, we propose the null hypotheses \mathcal{H}_0 and alternative hypotheses \mathcal{H}_1 are unchanged pixels and changed pixels, respectively. Hypotheses for change detection take the following form

$$\mathcal{H}_0: p(D(u, v)) > \tau \quad (13)$$

$$\mathcal{H}_1: p(D(u, v)) \leq \tau \quad (14)$$

where the threshold τ can be calculated by significance level α (Devore, 2011). The null distribution is modeled by Gaussian distribution with zero mean and variance σ^2 . (Aach, 1993, Aach, 1995). The variance σ^2 can be estimated from the unchanged region in the difference image $D(u, v)$. The Gaussian probability density function at pixel (u, v) is expressed

$$p(D(\bar{u}, \bar{v})) = \frac{1}{\sqrt{2\pi\sigma^2}} \exp\left(-\frac{D(\bar{u}, \bar{v})}{2\sigma^2}\right) \quad (15)$$

The block-wise formulation can ignore one changed pixel in an unchanged region and vice versa. We assume that the pixel in $\Omega_D(u, v)$ which square block of pixels centered at (u, v) in difference image $D(u, v)$, satisfies independent and identically distributed (iid). The block-wise formulation, which is based on Equation (15), can be expressed

$$p(D(u, v)) = \prod_{(\bar{u}, \bar{v}) \in \Omega_D(u, v)} \frac{1}{\sqrt{2\pi\sigma^2}} \exp\left(-\frac{D(\bar{u}, \bar{v})}{2\sigma^2}\right) \quad (16)$$

3. Results

3.1 Study area and data

We choose two study areas: (1) the village at the foot of volcano Fuego and (2) Southern California. The volcano Fuego erupted on June 3, 2018. The Formosat-2 image and the Formosat-5 image were acquired on October 5, 2012 and June 13, 2018, respectively. There were magnitude 7.1 and 6.4 earthquakes on July 5, 2019 and July 4, 2019 in Southern California, respectively. The Formosat-2 image and the Formosat-5 image were acquired on September 24, 2015 and July 12, 2019, respectively.

3.2 Analysis results

The Figure 1. (a) and (b) show the RGB bands image and NIR band image of Formosat-

2 image, respectively. The Figure 1. (d) and (e) show the RGB bands image and NIR band image of Formosat-5 image, respectively. The Figure 1. (c) shows the change mask. The Figure 1. (f) shows the change mask on the NIR band image of Formosat-5 image. This result shows that the village is submerged by lava.

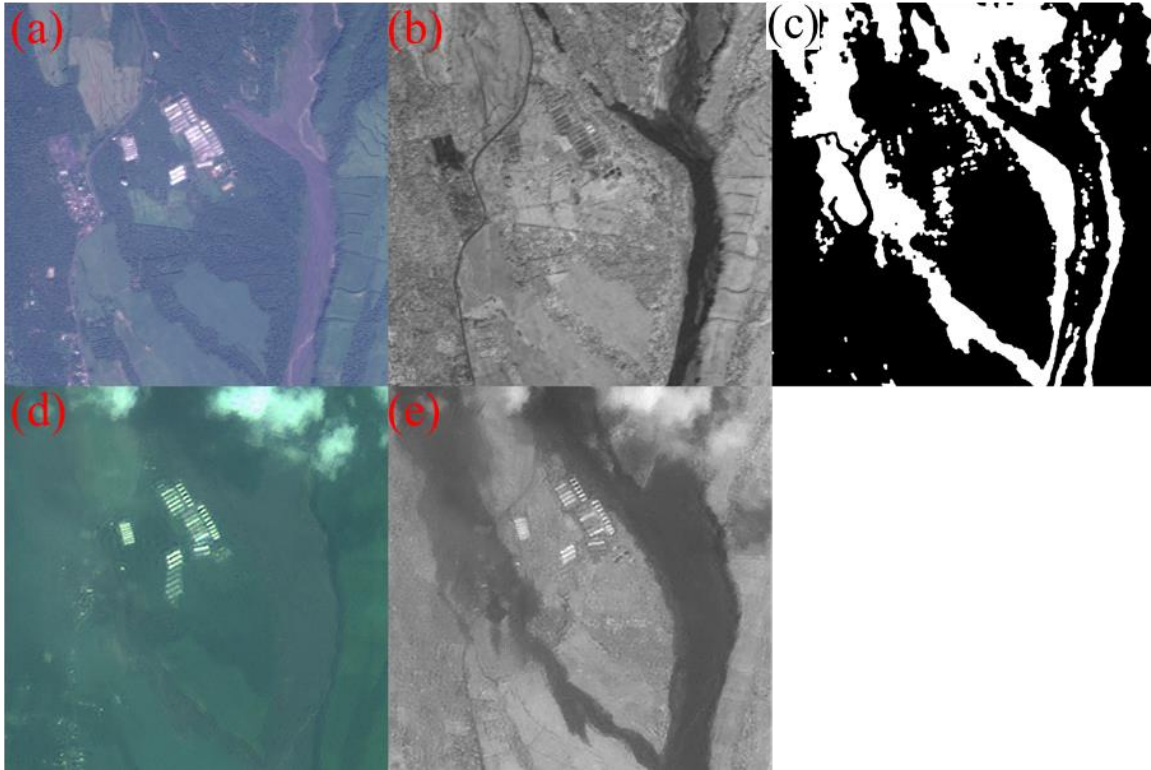


Figure 1. (a) and (b) show the RGB bands image and NIR band image of Formosat-2, respectively. (c) shows the change mask. (d) and (e) show the RGB bands image and NIR band image of Formosat-5, respectively.

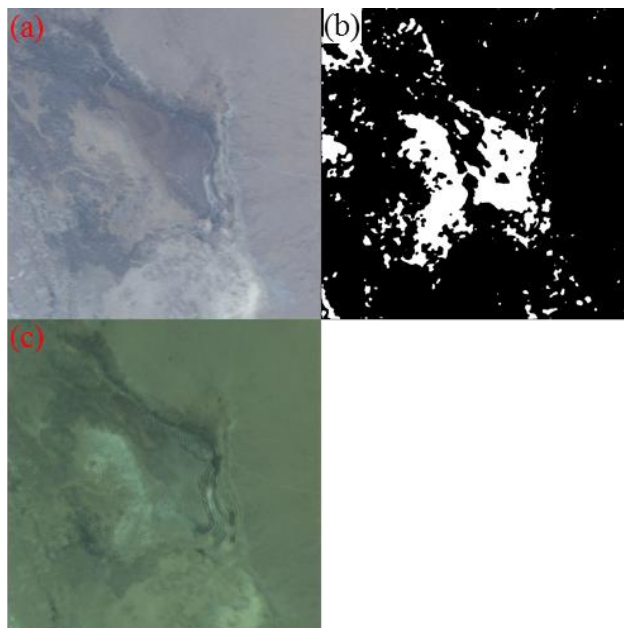


Figure 2. (a) shows the RGB bands image of Formosat-2. (b) shows the change mask. (c) shows the RGB bands image of Formosat-5.

The Figure 2. (a) shows the RGB bands of Formosat-2 image. The Figure 2. (c) shows the RGB bands of Formosat-5 image, respectively. The Figure 1. (b) shows the change mask. The Figure 1. (d) shows the change mask on the RGB bands image of Formosat-5. This result shows that the Southern California had large groundbreaking.

4. Conclusion

In this study, we propose a change detection method based on KL-div and hypothesis testing for Formosa satellite images. The results show this method can detect the large ground change between Formosat-2 images and Formosat-5 images. In a future work, we will consider image feature information into our method.

5. References

- Aach, T., and Kaup, A., 1993. Statistical model-based change detection in moving video. *Signal Processing*, 31 (2), pp. 165-180.
- Aach, T., and Kaup, A., 1995. Bayesian algorithms for adaptive change detection in image sequences using Markov random fields. *Signal Processing: Image Communication*, 7 (2), pp. 147-160.
- Bruzzone, L., and Prieto, D. F., 2002. An Adaptive Semiparametric and Context-Based Approach to Unsupervised Change Detection in Multitemporal Remote-Sensing Images. *IEEE Transactions Image Processing*, 11 (4), pp. 452-466.
- Collins, J. B., and Woodcock, C. E., 1996. An Assessment of Several Linear Change Detection Techniques for Mapping Forest Mortality Using Multitemporal Landsat TM Data. *Remote Sensing of Environment*, 56. Pp. 66-77.
- Dai, X., and Khorram, S., 1998. The effects of image misregistration on the accuracy of remotely sensed change detection. *IEEE transactions on geoscience and remote sensing*, 36 (5), pp. 1566-1577.
- Devore, J. L., 2011. *Probability and Statistics for Engineering and the Sciences*, Cengage Learning, Boston, pp. 300-344.
- Kullback, S., and Leibler, R. A., 1951. On information and sufficiency. *Annals of Mathematical Statistics*, 22 (1), pp. 76-86.
- Phong, B. T., 1975. Illumination for computer generated picture. *Communications of the ACM*, 18 (6), pp. 311-317. *Signal Processing: Image Communication*, 1 (2), pp. 191-212.
- Radke, R. J., Al-Kofahi, O., and Roysam, B., 2005. Image change detection algorithm:

A systematic survey. IEEE Transactions on Image Processing, 14 (3), pp. 294-307.

Rosin, P. L., 1998. Thresholding for change detection. In: Proceedings of International Conference on Computer Vision, Bombay, pp. 274-279.

Skifstad, K., and Jain, R., 1986. Illumination independent change detection for real world image sequences. Computer vision, graphic and image processing, 46 (3), pp. 387-399.

Toth, D., Aach, T., and Metzler, V., 2000. Illumination-Invariant Change Detection. In: 4th IEEE Southwest Symposium on Image Analysis and Interpretation, Austin, pp. 3-7.

Vermote, E., Tanre D., Deuze, J. L., Herman, M., Morcrette, J. J., and Kotchenova, S. Y., 2015. Second simulation of a satellite signal in the solar spectrum-vector (6SV) from http://6s.ltdri.org/files/tutorial/6S_Manual_Part_1.pdf